ORIGINAL ARTICLE

IWJ WILEY

Tissue chondrification and ossification in keloids with primary report of five cases

Qiannan Li [ID] | Tian Tu | Xiaoli Wu | Wenbo Wang | Zhen Gao | Wei Liu [ID]

Department of Plastic and Reconstructive Surgery, Shanghai Key Laboratory of Tissue Engineering Research, Shanghai Ninth People's Hospital, Shanghai Jiao Tong University School of Medicine, Shanghai, China

Correspondence
Wei Liu and Zhen Gao, Department of Plastic and Reconstructive Surgery, Shanghai Ninth People's Hospital, Shanghai Jiao Tong University School of Medicine, Shanghai Key Laboratory of Tissue Engineering Research, 639 Zhi Zao Ju Road, Shanghai 200011, China.
Email: liuwei_2000@yahoo.com (W. L.) and shgaozhen@126.com (Z. G.)

Present address
Qiannan Li, Department of Dermatology, Shuguang Hospital Affiliated to Shanghai University of Traditional Chinese Medicine, Shanghai, China

Tian Tu, Department of Plastic and Aesthetic Center, The First Affiliated Hospital, Collage of Medicine, Zhejiang University, Hangzhou, Zhejiang, China

Funding information
National Natural Science Foundation of China, Grant/Award Number: 81671921

Abstract

Keloid is commonly regarded as a benign skin tumour. Some keloids clinically exhibit hard tissue texture similar to that of cartilage or bone. We hypothesized that the keloid pathological niche environment is likely to induce keloid MSCs towards chondrogenic or osteogenic differentiation and leads to cartilage or bone-like tissue formation. The differences in tissue ossification, histology, mechanical properties, abnormal extracellular matrices and chondrogenic/osteogenic gene expression among sclerous keloids (SKs), regular keloids (RKs) and normal skins (NKs) were carefully examined. The sporadic ossified islets existed in SK group whereas no ossified/chondrified islet was found in other groups by micro-CT reconstruction. H&E, Masson trichrome and safranin O staining revealed lacuna-like structures in SKs, which were featured as bone/cartilage histology. Immunohistochemical staining showed overproduction of osteoprotegerin, type I and III collagen in SK group but similar production level of aggrecan among three groups. The biomechanical analysis demonstrated the weakest compliance of SK tissues. In addition, SK fibroblasts exhibited a relatively slower proliferation rate but higher expression levels of osteogenic and chondrogenic genes among all three groups. These cell populations also showed the strongest potential for lineage transformation. In conclusion, we first reported the presence of ossified and chondrified matrices in some extremely hard keloids in the present study.

KEYWORDS
cell transdifferentiation, heterotopic ossification, micro-CT screening, osteo/chondrogenic genes, sclerous keloid

Key Messages
- Keloid is a benign skin tumour characterised by excessive collagen deposition and fibroblast hyperproliferation
- This study demonstrates the presence of ossified and chondrified matrices in some extremely hard keloids

- Keloid pathological niche environment is likely to induce keloid stem cell differentiation towards chondrogenic and osteogenic lineages, and thus tissue ossification
- Further dissection of the underlying mechanism will help to design a proper therapeutic strategy for this type of keloids in the future

1 | INTRODUCTION

Keloid is commonly regarded as a benign skin tumour characterised by excessive collagen deposition and fibroblast hyperproliferation as well as an invasion into normal skin.[1] Keloids usually exhibit skin neoplasm with apparent redness or congestive appearance and symptom of pain and itching.[2] However, some keloids exhibit a hard tissue texture simulating cartilage or bone-like tissues, indicating the heterogenous origins of keloid formation.[3]

Although this phenomenon has been observed in the clinic, there are rarely reports on the investigation on this particular type of keloids with detailed histological, mechanical and genetic studies to prove the existence of osteogenesis in this type of keloids, despite that gene expression profile shifting to chondrocytic and osteogenic lineages were previously reported in keloid fibroblasts (KFs).[4] In addition, the presence of mesenchymal stem cells (MSCs) were also demonstrated in keloids, which had multiple differentiation potentials including chondrogenesis and osteogenesis,[5,6] suggesting the potential contribution of keloid stem cells to keloid chondrification and ossification.

The tissue environmental niche is the key factor for stem cells differentiation.[7,8] Based on the clinically observed phenomenon, we hypothesized that the keloid pathological niche environment is likely to induce keloid MSCs towards chondrogenic or osteogenic differentiation and lead to cartilage or bone-like tissue formation with a significant hardness of the tissue texture.

This study aimed to verify the proposed hypothesis by the analyses of micro-CT, histochemistry, cell expansion efficiency, tissue mechanical property and gene expression related to tissue chondrification and ossification as well as abnormal extracellular matrices to detect these differences among hard keloids, regular keloids and normal skins.

2 | MATERIALS AND METHODS

2.1 | Patients information and tissue samples

Total 15 patients (8 male and 7 female, age range 35-60 years, Table S1), including 5 patients of sclerous keloids (SKs), 5 patients of regular keloids (RKs) and 5 normal skin dermis (ND) donors. Briefly, these tissues were donated by patients/donors who received plastic surgery with written informed consent. Protocols for the handling of human tissues and cells were approved by the Ethics Committee of Shanghai Ninth People's Hospital affiliated to Shanghai Jiao Tong University, School of Medicine. The collected keloids were divided into hard keloids and normal keloids. The former had stuffiness similar to that of cartilage and was difficult to deform when applying pressure on them, whereas the latter was soft and easily deformed when pressure was applied.

2.2 | Micro-CT scanning and three-dimensional reconstruction

Tissue samples derived from NDs, RKs and SKs were evaluated for possible tissue ossification by micro-CT scanning (80 μ, Scanco Medical, Zurich, Switzerland). The regions of interest were the osteogenic area of the tested samples. The scanned data were reconstructed in Materialise's interactive medical image control system (Materialise, Belgium) to establish 3D images (Mean threshold value = 226). The ossified area was identified according to tissue density.

2.3 | Biomechanical property analysis

Briefly, mechanical properties (n = 5 for each group) of fresh tissue samples were evaluated from two dimensions (X-axes and Z-axes) by means of tensile or compressive tests using a biomechanical analyser (Instron 5542). The specimens were clamped into sample holders and continuous planar unconfined compressive tests were carried out at room temperature along the vertical direction (Z-axis) at a speed of 1 mm/min and a strain-rate of $0.033 \pm 0.0021/s$ up to the failure of the samples (turning point appears in the force-displacement curve). Compressive Young's modulus, as well as maximal force, was calculated according to the auto-generated force-displacement curves for statistical analysis. Maximum forces were recorded for statistical analysis.

2.4 | Histological analysis

The harvested tissue specimens were fixed in 4% paraformaldehyde in phosphate-buffered saline (PBS) overnight. After being dehydrated through a graded series of ethanol, the specimens were embedded in paraffin and cut into slices in 5-μm thickness as previously described.[9] The tissue slices were then stained with haematoxylin and eosin staining kit (H&E, Sigma, St. Louis, MO), Masson's Trichrome staining kit (Sigma, St. Louis, MO) and Safranin-O staining kit (Servicebio, Wu Han, China) to reveal the tissue morphology and osteochondral formation of each specimen.

2.5 | Immunohistochemical staining

According to a previous study,[10] after conventional deparaffinisation and rehydration of tissue sections, antigens were retrieved by microwave at 500 W for 2 to 5 minutes in 10 mM citrate buffer (pH 6.0). After being rinsed in Trisbuffered saline (pH 7.6), endogenous peroxidase activity was blocked in a solution of H_2O_2 (3%) followed by the addition of 5% rabbit serum (1:20 dilution in PBS, Boster, AR1010). Tissue samples were subsequently incubated with primary antibodies (listed in Table S2) in PBS overnight at 4°C. AfterPBS washes, samples were then incubated with horseradish peroxidase-conjugated secondary antibody (DAKO) for 30 minutes at 37°C. Target antigens were visualised by chemical substrate DAB (3,3-Diaminobenzidine, DAKO) and then counterstained with haematoxylin. Images were captured using Olympus IX70 microscope (Olympus, Center Valley, PA) and QCapture Pro 6.0 digital capture software.

2.6 | Isolation and culture of fibroblasts

The harvested normal skins and keloid tissues were collected in a 50-mL centrifuge tube, followed by three washes in 2.5% chloramphenicol solution for 5 minutes each time. Then the tissues were soaked in PBS for 5 minutes. Afterwards, the epidermis was removed by a scalpel, and the remaining dermis was minced into small pieces followed by enzyme digestion with collagenase NB4 (SERVA Electrophoresis, Heidelberg, Germany) dissolved in Dulbecco's modified Eagle's medium (DMEM, Hyclone, USA) for 4 hours at 37°C on a rotator. After digestion, the collected cells were centrifuged at 1500 rpm for 5 minutes and then resuspended in DMEM supplemented with 10% fetal bovine serum (FBS) and penicillin/streptomycin. The cells were seeded onto a 10-cm culture dish at a density of 2×10^4 cells/cm^2 and cultured in a humidified 5% CO_2 atmosphere at 37°C. When the cells reached 90% confluence, they were detached with 0.25% trypsin EDTA and subcultured at the same density. Passage 3 or 4 cells were used for *in vitro* osteogenic, chondrogenic and adipogenic differentiation experiments, while the primary and first passage cells were used in the other experiments.

2.7 | CCK-8 cell proliferation assay

The fibroblasts derived from normal skin and keloids were respectively seeded in 96-well plates with 1000 cells per well along with 200 μL of the medium. After being starved in a serum-free medium for 24 hours to allow for cell synchronisation, the cells were replaced with fresh culture medium regularly and then tested with a cell counting kit-8 (CCK-8; Dojindo, Japan) at days 1, 3, 5, and 7. Briefly, at each testing time point, 10 μL of sterile CCK-8 solution was added to each well and incubated for 2 hours at 37°C, and then the medium was harvested for measuring the optical density values at 450 nm via a microplate reader (Thermo Scientific). All the assays were performed in quintuplicate and repeated using three cell samples.

2.8 | RNA extraction and real-time quantitative polymerase chain reaction (qPCR)

Total RNA was extracted from the cells using Trizol Reagent (Invitrogen, Carlsbad, CA) without detaching the cells. The complementary DNA (cDNA) was synthesised from 2 μg total RNA per sample with AMV reverse transcriptase (Takara, Japan) in a 20-μL reaction solution containing 4 μL 5× buffer, 2 μL dNTP, 1 μL oligo-(dT), 0.5 μL RNase inhibitor and 0.5 μL AMV reverse transcriptase and ddH_2O. The mixture was then incubated at 30°C for 10 minutes, 42°C for 60 minutes, 95°C for 5 minutes and 5°C for 5 minutes.

Then, cDNA was amplified using a Power SYBR Green PCR master mix (×2) (Applied Biosystems, Foster City, CA) in a real-time thermal cycler (Stratagene Mx3000PTM QPCR System, La Jolla, CA), and each measurement was repeated in triplicate. The optimised primers for qPCR analysis were listed in Table S3. The human housekeeping gene *Hypoxanthine phosphoribosyl transferase 1* (*HPRT1*) was used as an internal control. Experiments were repeated in three cell samples.

2.9 | *In vitro* osteogenic, chondrogenic and adipogenic induction of fibroblasts

Induction of multilineage differentiation on the fibroblasts derived from three tissue types was performed by

using commercially available chondrogenic, adipogenic and osteogenic induction media according to the manufactures protocol (Lonza) and previous studies.[11-13] Osteogenic induction medium was composed of L-glutamine (1%) ascorbate (50 μM), penicillin–streptomycin (1%), β-glycerophosphate (10 mM) and dexamethasone (0.1 μM). Adipogenic induction medium was composed of h-insulin (5 μg/mL), L-glutamine (1%), dexamethasone (1 μM), indomethacin (0.1 μM), 3-isobutyl-1-methyl-xanthine (0.5 mM), penicillin–streptomycin (1%). Chondrogenic induction medium was composed of ascorbate (0.17 mM), ITS$^+$ supplement, dexamethasone (0.1 μM), penicillin–streptomycin (1%), sodium pyruvate (1 mM), proline (1 mM), L-glutamine (1%) and transforming growth factor-β3 (TGF-β3, 0.01 μg/mL). The medium was changed at 3-day intervals.

2.10 | Phenotype characterisation and quantitative analyses

The adipogenic phenotype was assayed by Oil Red O staining. To stain lipids, cells were exposed to a working solution of Oil Red O (3 mg/mL in 99% isopropanol,

Sigma) and the background was cleared with 60% isopropanol.

The osteogenic differentiation was determined by staining for Alizarin Red S. Cells cultured under osteogenic differentiation conditions were fixed at the different time points with a 10% formalin solution and washed, first with PBS, and then with diH$_2$O. The cells were then incubated for 10 minutes with a 2% (wt/v) Alizarin Red S solution (Sigma) in diH$_2$O, at a pH of 4.1 to 4.3. After incubation, cells were washed again with diH$_2$O and the staining was observed under a stereo microscope Stemi 1000 (Zeiss).

To observe chondrogenic differentiation of cells, Toluidine Blue staining was performed as described previously.[12] Briefly, after 6 days of micromass culture, cell pellets were rinsed with PBS and then fixed with 10% (v/v) formalin containing 0.5% (w/v) cetylpyridinium chloride (CPC) for 10 minutes at room temperature. After being rinsed with 3% (v/v) glacial acetic acid (pH 1.0), cell pellets were then incubated in 1 mL of 0.5% (w/v) Alcian blue 8GX (Sigma) in 3% (v/v) glacial acetic acid (pH 1.0) overnight at room temperature. As described,[11] semi-quantitative analysis of the multilineage differentiation was performed by measuring the total area of
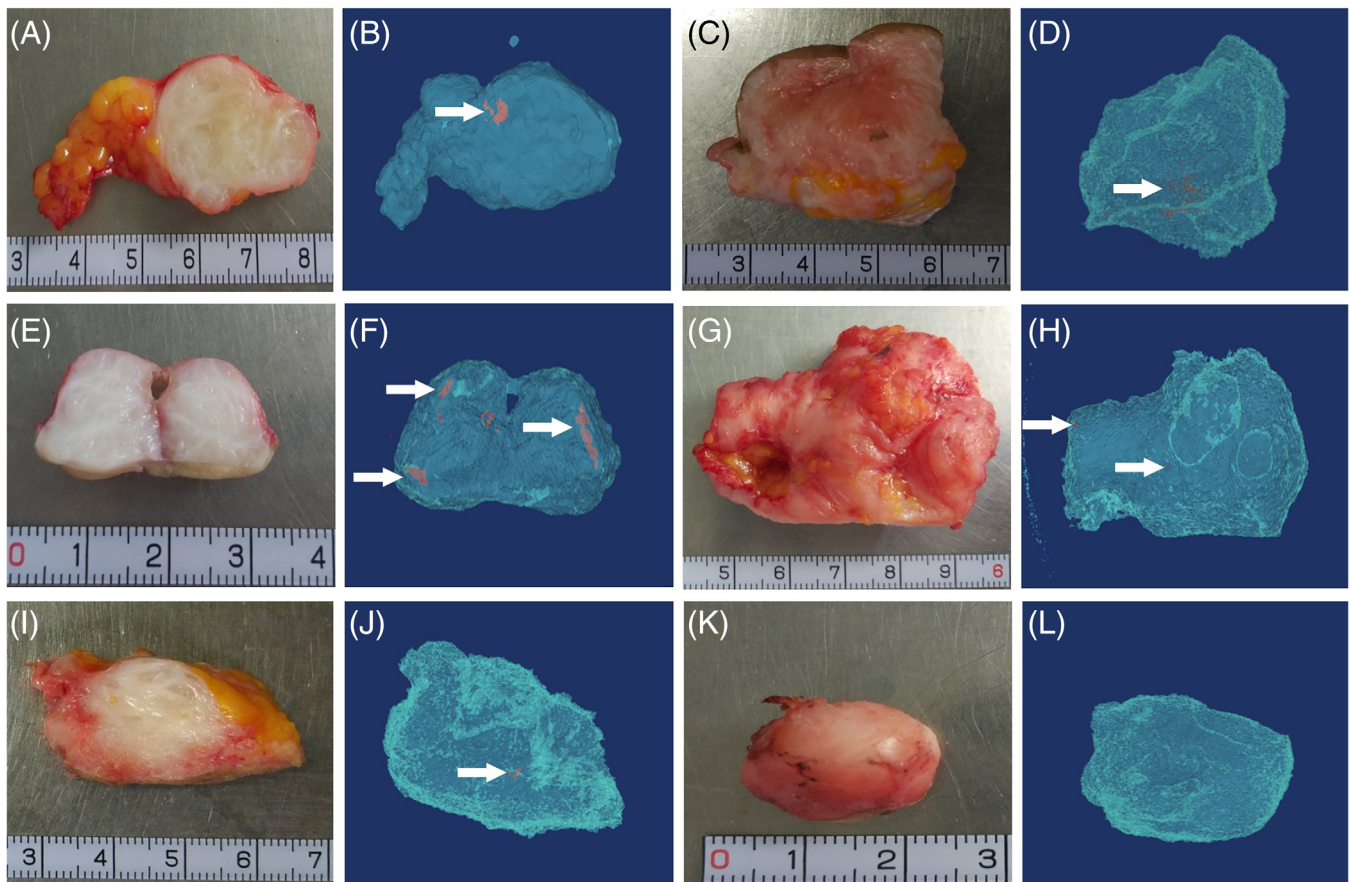

FIGURE 1 Keloid gross view and the corresponding micro-CT images of calcified tissue. Gross view of all five sclerous keloids (A, C, E, G and I) and their corresponding 3D reconstruction of micro-CT images (B, D, F, H and J) that reveal the presence of ossified islets (white arrowed). No ossified islet is found in the regular keloid tissue as demonstrated by reconstruction of micro-CT image (K and L)

multilineage differentiation from each group (n = 5) using ImageJ software (version 1.8.0; National Institutes of Health).

2.11 | Statistical analysis

All data were presented as mean ± standard deviation. Significance was evaluated by one-way analysis of variance test then a Least Significant Difference post-hoc test using SPSS version15.0 (IBM, Armonk, NY). A P-value of less than .05 was considered to indicate a statistically significant difference.

3 | RESULTS

3.1 | Ossified extracellular matrix was identified in sclerous keloid tissue samples

To verify if ossified/chondrified matrix was presented in keloid samples, five sclerous keloid samples and five regular keloid tissues were evaluated with micro-CT analysis. The CT images of keloid tissues were reconstructed in a 3D level, where fibrosis tissue with different tissue densities was visualised by diverse colour depths. Ossified extracellular matrix with a significantly higher CT value was identified as indicated by white arrows (Figure 1). The reconstructed μCT images demonstrated that sporadic ossified islets existed in all five sclerous keloid tissues (Figure 1A-J) whereas no ossification was found in all regular keloid tissues (Figure 1K,L). These ossified islets were found to be positioned at both the central and marginal areas of sclerous keloids with irregular shapes.

3.2 | Histological comparison among NDs, RKs and SKs

H&E, Masson trichrome and safranin O staining were employed to evaluate the differences in histological structure and particular extracellular matrix among NDs, RKs and SKs. As illustrated in Figure 2A, SKs contained the
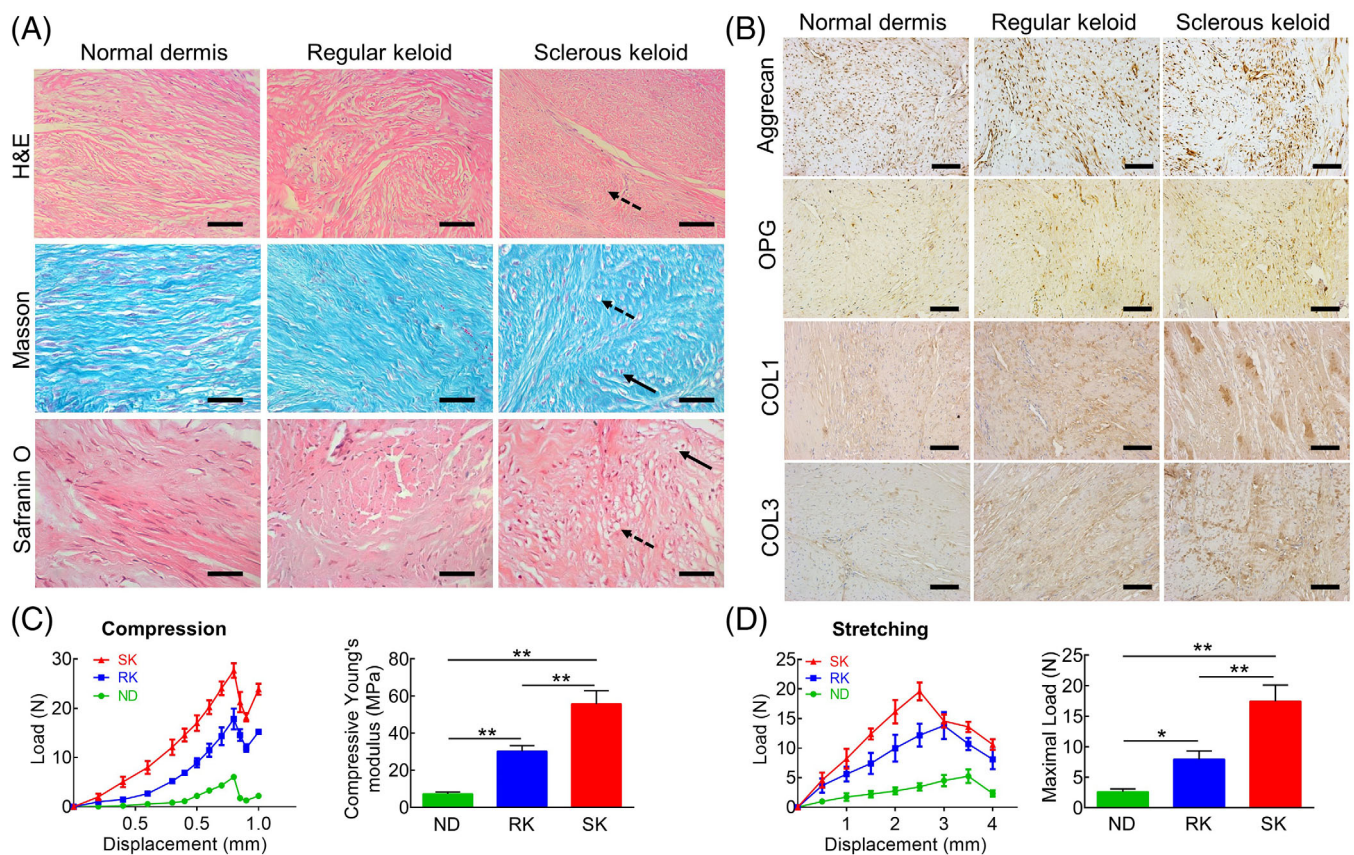

FIGURE 2 Histological and biomechanical analyses of normal skin dermis (ND), regular keloid (RK) and scelrous keloid (SK) tissues. (A) Relatively denser collagen fibres and lacuna-like structure are found in SK as revealed by H&E staining, Masson staining and safranin O staining. Dotted arrows indicate the presence of lacuna-like structure in SK tissues, whereas the solid arrows indicate the enlarged cell nuclei. Magnification = ×200; Bar = 100 μm. (B) Immunohistochemical staining shows abnormal ECM deposition where excessive OPG, COL1 and COL3 are observed in SK tissue compared to other tissue types. Magnification = ×200; Bar =100 μm. (C and D) Compressive Young's modulus and maximal loading are respectively presented with quantification analysis of ND, RK and SK tissues, which show significant differences among three groups. *$P < .05$, **$P < .01$

densest but the thinnest collagen fibres and nearly no blood vessels. Interestingly, H&E examination revealed that bone/cartilage-lacunas-like structure was observed in SKs (dotted arrow), but not in RKs or NSs. Moreover, Safranin O and Masson staining showed that not only the lacuna-like structures (dotted arrow), but also bigger and round cell nucleus (solid arrow) were found in SKs compared to RKs and ND (Figure 2A).

Immunohistochemical staining also revealed a similar phenomenon. As shown, stronger staining of osteoprotegerin (OPG), a protein usually expressed in mature osteoblasts,[14] was presented in keloid tissues compared to the normal dermis and was even higher in SKs as visually observed (Figure 2B). Similar patterns could also be observed when investigating the deposition of type I and III collagen (Figure 2B). However, no significant alteration regarding aggrecan production, one of the cartilage-specific extracellular matrix (ECM) components, was observed among three groups (Figure 2B).

3.3 | Ossification/chondrification attenuated compliance of sclerous keloid scars

Compliance of skin is considered as an important parameter for evaluating the severity of fibrosis disease. To demonstrate the weakened compliance of SKs, a biomechanical analysis was performed (Figure 2C). Both the maximum loading force and compressive Young's modulus were significantly higher in KSs than in RKs and NDs with significant differences among the three groups. The lowest maximum loading force and compressive Young's modulus were observed in the normal dermis. Among three different types of tissues, the biggest force is needed to stretch SKs for the same distance when they were subject to mechanical tests (Figure 2D).

3.4 | Chondrification/ossification attenuated keloid fibroblast proliferation potential

To determine the effect of potential ossification or chondrification on keloid fibroblasts (KFs) proliferation, a CCK-8 assay was performed. As shown, normal fibroblasts (NFs), KFs and sclerous keloid fibroblasts (SKFs) showed different proliferation curves under the same culture condition (Figure 3A). Among these groups, the SKFs proliferated faster than NFs but slower than KFs.

3.5 | Enhanced gene expression of ossification/chondrification markers in SKFs

The gene-level of chondrogenic/osteogenic markers were also investigated among three groups. As shown, genes
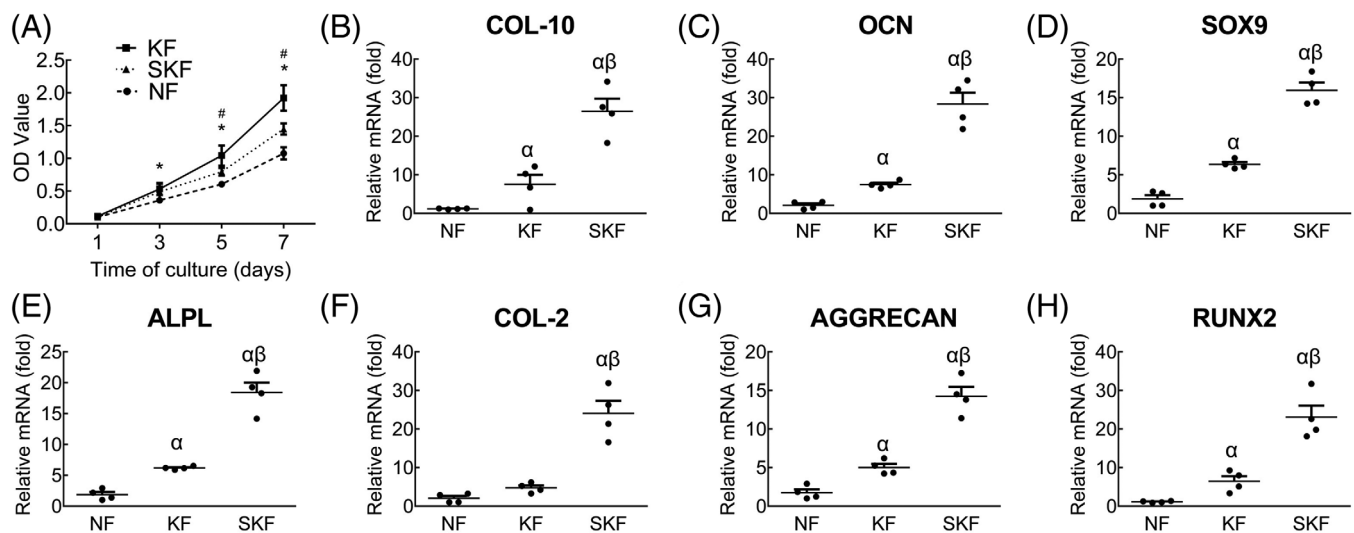

FIGURE 3 Cell proliferation and chondrogenic and osteogenic gene expressions in ND fibroblasts (NFs), RK fibroblasts (KFs) and SK fibroblasts (SKFs). (A) CCK-8 assay reveals that both SKFs and KFs proliferate faster than NFs, and SKFs are attenuated for their proliferation potential. #, significant difference between SKFs and NFs groups ($P < .05$). *, significant difference between KFs and NFs ($P < .05$). (B-H) Elevated expression levels of genes related to osteogenic and chondrogenic differentiation are detected via qPCR. α, significant difference between KFs and NFs ($P < .05$). β, significant difference between SKFs and KFs and between SKFs and NFs ($P < .05$)

related to osteogenic and chondrogenic differentiation such as *type X collagen* (COL10, Figure 3B), *osteocalcin* (OCN, Figure 3C), *SRY-box 9* (SOX-9, Figure 3D), *alkaline phosphatase* (ALPL, Figure 3E), *type II collagen* (COL2, Figure 3F), *aggrecan* (Figure 3G), and *runt-related transcription factor 2* (RUNX2, Figure 3H) were all up-regulated in SKFs with a significant difference when compared with NFs or KFs (Figure 3B-H, $P < .05$). Typically, the expression levels of these genes in KFs were relatively higher than those of NFs except for the expression level of *COL2* (Figure 3F, $P < .05$).

3.6 | SKFs exhibited stronger differentiation potentials towards chondrogenic, osteogenic and adipogenic lineages

To examine the difference in multilineage differentiation potentials among three groups, a comparison on trilineage marker expression was performed by phenotype characterisation. As shown, after 10 days of osteogenic induction,

21 days of chondrogenic and adipogenic induction, much more potent osteogenesis, chondrogenesis and adipogenesis were found in the induced SKF group compared to other two induced groups when evaluated with histochemical staining (Figure 4A). Semi-quantification analysis also showed the strongest potentials of SKFs among all three groups, and KFs also showed stronger potentials than NFs (Figure 4B).

4 | DISCUSSION

Keloid is commonly considered as a benign skin fibrosis disorder or a benign skin tumour that is often seen in Asians and Africans with excessive collagen deposition and aberrant fibroblast hyperproliferation.[15] As generally acknowledged, keloid lost its original tissue compliance during the progression due to the uncontrolled deposition of extracellular matrix.[16]

As a fibrotic skin disease, keloids usually behave as a soft tissue neoplasm.[17] However, some stiffened keloids were usually observed in earlobe, shoulder and other
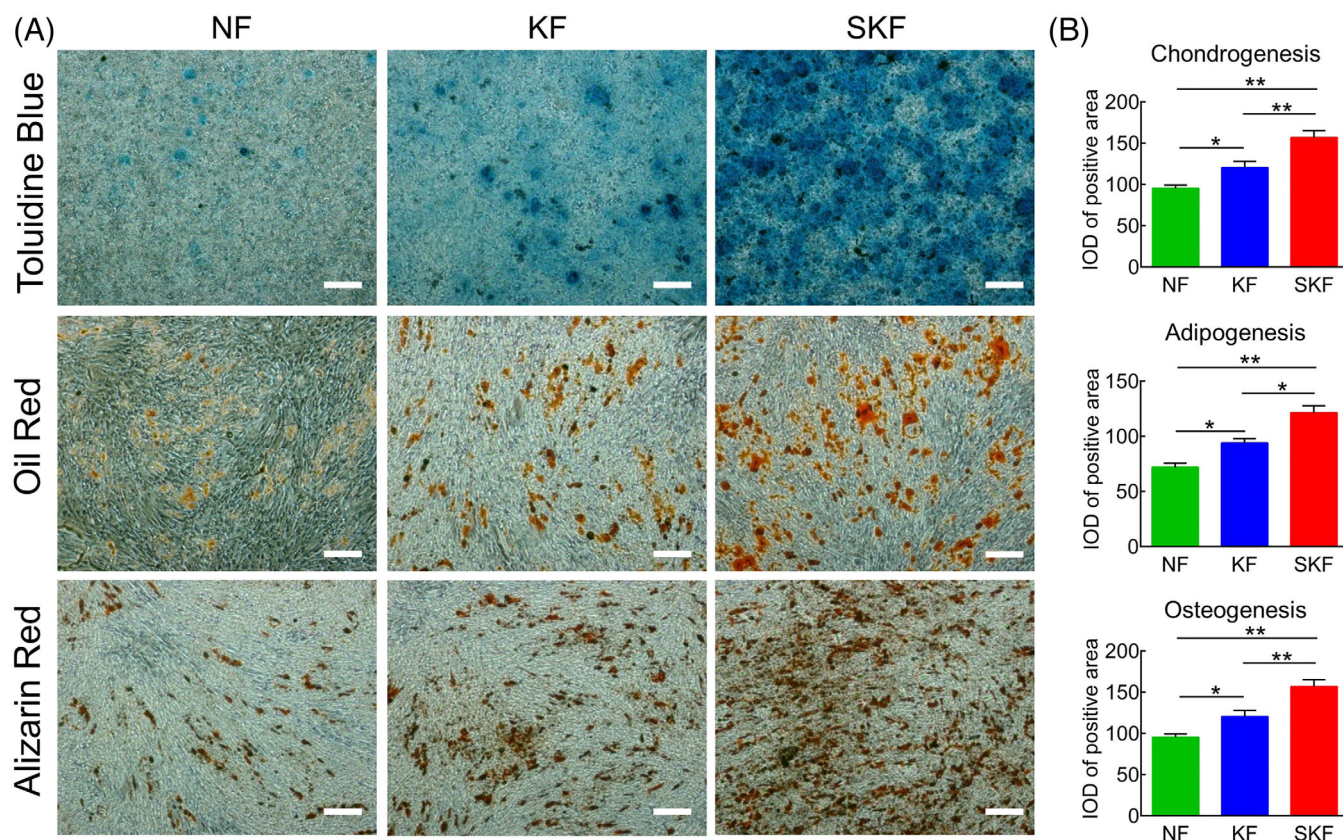

FIGURE 4 In vitro evaluation of differentiation potential of NFs, KFs and SKFs. (A) Histochemistry of Toluidine blue, Oil Red and Alizarin Red staining are employed to respectively evaluate chondrogenic, adipogenic and osteogenic differentiation potentials of all three groups cells. Magnification = ×40; Bar = 250 μm. B. Semi-quantitation of IOD of positive areas in each group is illustrated as histograms. IOD, integral optical density. *$P < .05$, **$P < .01$

locations with stiffness resembling cartilage or even bone, suggesting the diversity of keloid pathogenesis.[18] Although not reported in keloids as yet, tissue calcinosis has been observed in some skin diseases with significantly enhanced stiffness of subcutaneous extracellular matrices.[3,19,20] In addition, keloid fibroblasts have been shown to have transdifferentiation potential towards other lineages.[21] Thus, it would be interesting to investigate whether keloid tissue could be transformed into calcified tissues or cartilage-like tissue with cellular evidence of chondrogenesis and osteogenesis.

To proceed, sclerous keloids located at a mechanical-loading position, shoulder and prothoracic keloid samples were harvested from surgical procedures and subject to micro-CT analysis to demonstrate the presence of calcified matrix of keloid subcutaneous tissue. Interestingly, micro-CT did demonstrate the presence of a minor area of calcified islets in all five sclerous keloids, but none in regular keloids as shown in Figure 1.

Other than the abnormal radiologic characteristics, histological features of sclerous keloid tissues were also different from those of soft keloids. Logically, lacuna-like structures are universally observed in bone and cartilage. However, this characteristic structure was also observed in these sclerous keloid samples (Figure 2A). Furthermore, immunohistochemical staining revealed the overproduction of OPG, one of the representative components of bone ECM (Figure 2B).

Alteration in histological characteristics will inevitably lead to the changed tissue mechanical properties.[22] To confirm the stiffness differences among NDs, RKs and SKs, their maximal loading and compressive Young's modulus were measured. As shown in Figure 2C,D, significantly higher maximal loading and compressive Young's modulus were observed in SK group. All these evidences revealed in this study support the fact that SKs contain cartilage or bone-like tissues with transformed histological features and enhanced tissue stiffness, but the origination of heterogenous ECM remains unknown.

Previous studies revealed the presence of keloid mesenchymal stem cells, which were able to differentiate into several mesenchymal lineages such as osteoblasts and chondrocytes.[6,7] In addition, even unsorted keloid fibroblasts presented more potent differential potential than normal dermal fibroblasts.[7] Therefore, cellular functions were also investigated. As shown in Figure 3, even cultured under regular conditions without specific induction, SKFs expressed the highest levels of chondrogenic and osteogenic markers among all three groups, which also provided molecular evidence of the presence of calcified keloids. Interestingly, KFs also expressed higher levels of these markers than normal dermal fibroblasts, which was in agreement with a previous report.[4] On the other hand, attenuated proliferative capability may serve as a commitment of stem cell differentiation.[23-25] In the present study, it was revealed that SKFs exhibited a relatively slower proliferation rate as well as higher expression levels of osteogenic and chondrogenic genes. The *in vitro* experiments of this study also proved this phenomenon again, suggesting the stronger differentiation tendency of SKFs.

The molecular mechanism of ossified keloids remains less reported. Recently, keloid-derived precursor/stem cells and their inflammatory niche driven by IL-17/IL-6 axis were identified successfully, which provides a new hint to discover the source of the heterogenous matrix.[7] As widely known, various cytokines including IL-6, IL-8, and IL-10, as well as various growth factors such as TGF-β1 have been implicated in keloids.[26] Osteogenic and chondrogenic potentials of these precursor/stem cells might happen when cells were exposed to enriched intralesional cytokines and diverse specific growth factors.[27,28] It is likely that during the pathogenic process of keloid development, the aberrant production of several cytokines and growth factors might constitute an abnormal niche environment that promoted differentiation/transdifferentiation of keloid stem cells or keloid fibroblasts into chondrocytes or osteoblasts, which further produce cartilage or bone-related matrices.

Mechanical stimulation is also known for its promoting effect on chondrogenic or osteogenic differentiation of MSCs.[29,30] It is well known that keloids tend to form in the body areas that are subject to increased skin tension or stiffness, such as the prothoracic area and shoulders.[18] The dysfunction of cell mechanical sensing may elucidate the ectopic osteogenesis in keloids. The caveolin-1, one of the key molecules in the mechanosensation and mechanotransduction of cells, was attenuated in the keloid central area but was enhanced in its periphery tissues.[16] It was also found related to keloid peripheral mechanical stress and tissue stiffness during keloid progression and invasion.[31] In addition, its down-regulation may mediate the activation of ROCK pathway and enhanced expression of osteogenic gene RUNX2 in keloid fibroblasts.[16,31] In subsequent studies, amelioration of hyperresponsiveness to the mechanical stimuli could be realised by restoring caveolin-1 and its downstream signalling molecules.

In summary, the presence of ossified and chondrified matrices in some extremely hard keloids was the first report by this study. Some matrix components and structures that are similar to cartilage and bone tissues were observed in these sclerous keloid samples. The transdifferentiation potential of fibroblasts derived from SK tissues was also significantly enhanced. These results suggest that the pathological tissue environment constituted with aberrant cytokines and growth factors in keloids

may drive the keloid stem cells to differentiate towards other lineages and thus cause the enhanced tissue stiffness as seen in clinical hard keloids. Further mechanism exploration will help to design a proper therapeutic strategy for this type of keloids.

5 | CONCLUSION

In this study, we first reported the presence of ossified and chondrified matrices in some extremely hard keloids, suggesting the diversity of keloid pathogenic manifestations. Keloid pathological niche environment is likely to induce keloid stem cell differentiation towards chondrogenic and osteogenic lineages, and thus tissue ossification. An efficient therapeutic strategy will be developed given a further defined mechanism, which can help to develop an anti-scarring therapy for this type of keloids.

CONFLICT OF INTEREST
The authors declare no conflicts of interest.

AUTHOR CONTRIBUTIONS
Qiannan Li: Conceptualization, Methodology, Investigation, Visualisation, Writing - original draft. Tian Tu: Software, Writing - original draft, Writing - Review & Editing. Wenbo Wang: Validation, Methodology. Xiaoli Wu: Resources (Clinically relevant), Formal analysis; Zhen Gao: Formal analysis, Data Curation; Wei Liu: Conceptualization, Project administration, Supervision, Validation, Writing - Review & Editing, Funding acquisition.

DATA AVAILABILITY STATEMENT
Data openly available in a public repository that issues datasets with DOIs.

ORCID
Qiannan Li 🔟 https://orcid.org/0000-0003-1352-4105
Wei Liu 🔟 https://orcid.org/0000-0003-0508-4605

REFERENCES
1. Ghazawi FM, Zargham R, Gilardino MS, Sasseville D, Jafarian F. Insights into the pathophysiology of hypertrophic scars and keloids. *Adv Skin Wound Care*. 2018;31(1):582-595.
2. Niyaz A, Matsumura H, Watanabe K, Hamamoto T, Matsusawa T. Quantification of the physical properties of keloid and hypertrophic scars using the Vesmeter novel sensing device. *Int Wound J*. 2012;9(6):643-649.
3. Palumbo C, Ferretti M, Bonucci P, et al. Two peculiar conditions following a coma: a clinical case of heterotopic ossification concomitant with keloid formation. *Clin Anat*. 2008;21(4):348-354.
4. Naitoh M, Kubota H, Ikeda M, et al. Gene expression in human keloids is altered from dermal to chondrocytic and osteogenic lineage. *Genes Cells*. 2005;10(11):1081-1091.
5. Moon JH, Kwak SS, Park G, Jung HY, You S. Isolation and characterization of multipotent human keloid-derived mesenchymal-like stem cells. *Stem Cells Dev*. 2008;17(4):713-724.
6. Lim KH, Itinteang T, Davis PF, Tan ST. Stem cells in keloid lesions: a review. *Plast Reconstr Surg Glob Open*. 2019;7(5): e2228.
7. Zhang Q, Takayoshi Y, Paul KA, et al. Tumor-like stem cells derived from human keloid are governed by the inflammatory niche driven by IL-17/IL-6 axis. *PLoS One*. 2009;4(11): e7798.
8. Gonzales K, Fuchs E. Skin and its regenerative powers: an alliance between stem cells and their niche. *Dev Cell*. 2017;43(4): 387-401.
9. Huang J, Tu T, Wang W, et al. Aligned topography mediated cell elongation reverses pathological phenotype of in vitro cultured keloid fibroblasts. *J Biomed Mater Res A*. 2019;107(7): 1366-1378.
10. Tu T, Huang J, Lin M, et al. CUDC-907 reverses pathological phenotype of keloid fibroblasts in vitro and in vivo via dual inhibition of PI3K/Akt/mTOR signaling and HDAC2. *Int J Mol Med*. 2019;1(44):1789-1800.
11. Wang Z, Wu D, Zou J, et al. Development of demineralized bone matrix-based implantable and biomimetic microcarrier for stem cell expansion and single-step tissue-engineered bone graft construction. *J Mater Chem B*. 2017;5(1):62-73.
12. Barry F, Boynton RE, Liu B, Murphy JM. Chondrogenic differentiation of mesenchymal stem cells from bone marrow: differentiation-dependent gene expression of matrix components. *Exp Cell Res*. 2001;268(2):189-200.
13. Teven CM, Liu X, Hu N, et al. Epigenetic regulation of mesenchymal stem cells: a focus on osteogenic and adipogenic differentiation. *Stem Cells Int*. 2011;2011(1):1-18.
14. Rochette L, Meloux A, Rigal E, Zeller M, Cottin Y, Vergely C. The role of osteoprotegerin and its ligands in vascular function. *Int J Mol Sci*. 2019;20(3):705.
15. Unahabhokha T, Sucontphunt A, Nimmannit U, Chanvorachote P, Yongsanguanchai N, Pongrakhananon V. Molecular signalings in keloid disease and current therapeutic approaches from natural based compounds. *Pharm Biol*. 2015; 53(3):457-463.
16. Hsu CK, Lin HH, Harn IC, Ogawa R, Tang MJ. Caveolin-1 controls hyperresponsiveness to mechanical stimuli and Fibrogenesis-associated RUNX2 activationin keloid fibroblasts. *J Invest Dermatol*. 2018;138(1):208-218.
17. Huang C, Ogawa R. The vascular involvement in soft tissue fibrosis—lessons learned from pathological scarring. *Int J Mol Sci*. 2020;21(7):2542.
18. Ogawa R, Akaishi S, Huang C, Dohi T, Aoki Momori Y, et al. Clinical applications of basic research that shows reducing skin tension could prevent and treat abnormal scarring: the importance of fascial/subcutaneous tensile reduction sutures and flap surgery for keloid and hypertrophic scar reconstruction. *J Nippon Med Sch*. 2011;78(2):68-76.
19. Valenzuela A, Chung L. Calcinosis: pathophysiology and management. *Curr Opin Rheumatol*. 2015;27(6):542-548.

LI ET AL.

IWJ—WILEY | 1869

20. Franzen M, Moré E, Cadamuro J, et al. Mineral depositions of calcifying skin disorders are predominantly composed of carbonate apatite. *Acta Derm-Venereol*. 2017;97(10):1178-1181.
21. Plikus MV, Guerrero-Juarez CF, Ito M, et al. Regeneration of fat cells from myofibroblasts during wound healing. *Science*. 2017;355(6326):748-752.
22. Knecht S, Vanwanseele B, Stussi E. A review on the mechanical quality of articular cartilage - implications for the diagnosis of osteoarthritis. *Clin Biomech*. 2006;21:999-1012.
23. Reichert M, Eick D. Analysis of cell cycle arrest in adipocyte differentiation. *Oncogene*. 1999;18(2):459-466.
24. Ali D, Alshammari H, Vishnubalaji R, et al. CUDC-907 promotes bone marrow adipocytic differentiation through inhibition of histone deacetylase and regulation of cell cycle. *Stem Cells Dev*. 2017;26(5):353-362.
25. Tu T, Shen Y, Wang X, et al. Tendon ECM modified bioactive electrospun fibers promote MSC tenogenic differentiation and tendon regeneration. *Appl Mater Today*. 2020;18(1):100495.
26. Berman B, Maderal A, Raphael B. Keloids and hypertrophic scars: pathophysiology, classification, and treatment. *Dermatol Surg*. 2017;43(1):S3-S18.
27. Han J, Menicanin D, Gronthos S, Bartold PM. Stem cells, tissue engineering and periodontal regeneration. *Aust Dent J*. 2014;59(1):117-130.
28. Ullah I, Subbarao R, Rho G. Human mesenchymal stem cells - current trends and future prospective. *Biosci Rep*. 2015;35(2):1-18.
29. Fahy N, Alini M, Stoddart MJ. Mechanical stimulation of mesenchymal stem cells: implications for cartilage tissue engineering. *J Orthop Res*. 2017;1(36):52-63.
30. Wang J, Wang CD, Zhang N, Tong WX, Li QF. Mechanical stimulation orchestrates the osteogenic differentiation of human bone marrow stromal cells by regulating HDAC1. *Cell Death Dis*. 2016;7(5):e2221.
31. Dohi T, Padmanabhan J, Akaishi S, et al. The interplay of mechanical stress, strain, and stiffness at the keloid periphery correlates with increased Caveolin-1/ROCK signaling and scar progression. *Plast Reconstr Surg*. 2019;144(1):58e-67e.

SUPPORTING INFORMATION

Additional supporting information may be found in the online version of the article at the publisher's website.

How to cite this article: Li Q, Tu T, Wu X, Wang W, Gao Z, Liu W. Tissue chondrification and ossification in keloids with primary report of five cases. *Int Wound J*. 2022;19(7):1860-1869. doi:10.1111/iwj.13792